

where for conduction:

- C is the thermal capacity
- K is the thermal conductance
- Q is the heat addition or absorption
- t is time.

The conduction in the machine walls equation (2.4) is used without modification. However, to describe the energy transfer to a gas node the analogue suggested is shown in Figure 2.5. Here the C.F. nodes define enthalpy fluxes conditional on the mass flow direction.

Conditional temperatures for the enthalpy terms are used. This works on the principle that if gas is flowing out of a node, then it flows out at the nodal temperature. If however gas flows into a node, then it flows in at its immediate upstream temperature.

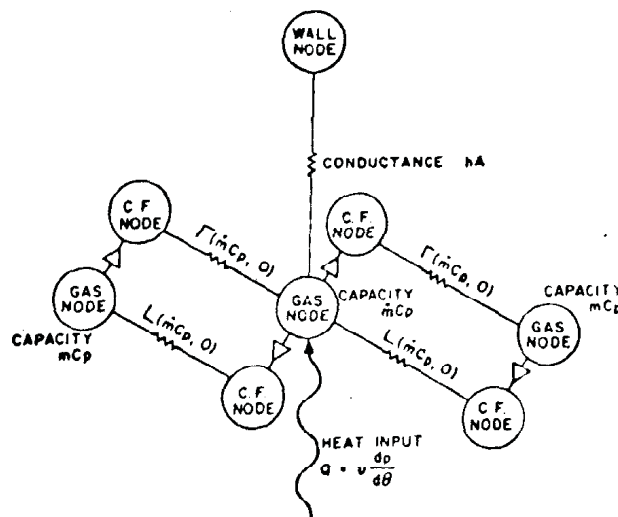


Figure 2.5 The Gas Node (after Finkelstein[Fi75])

Finkelstein indicates that one computational cycle took about twelve minutes computing time on an IBM 360/65. It is not

Indicated whether this is CPU time or total time in the computer, but however, it indicates that this programme is very expensive to run.

An interesting point arises when considering the simulation of Stirling refrigerators or cryogenerators. Since these machines work at very much lower temperatures than engines, the local speed of sound will be slower. The local speed of sound is given by [Jo71]:

$$C = \sqrt{\gamma R T} \quad (2.5)$$

where

- γ is the ratio of the specific heats
- T is the local gas temperature
- R is the gas constant.

From (2.5) it can be expected that low temperature cryogenerators may well operate with the working gas velocities approaching sonic conditions. Flow induced compressibility effects start becoming important at about a Mach number of 0,2. It thus appears that compressibility effects should be properly accounted for in such simulation work and this would necessitate accurate modelling of the gas momentum.

2.6 Urieli's Model

Urieli *et al* [UR77] presented a Stirling machine simulation model in September 1977 at the 12th IECEC. This was a report of the work done whilst Urieli was enrolled for a PhD at the Witwatersrand University [Ur77].

Urieli tackled the problem by subdividing the Stirling machine into a variable number of cells (Figure 2.6). The three fundamental transport equations (continuity, momentum and energy)

were applied to each individual cell.

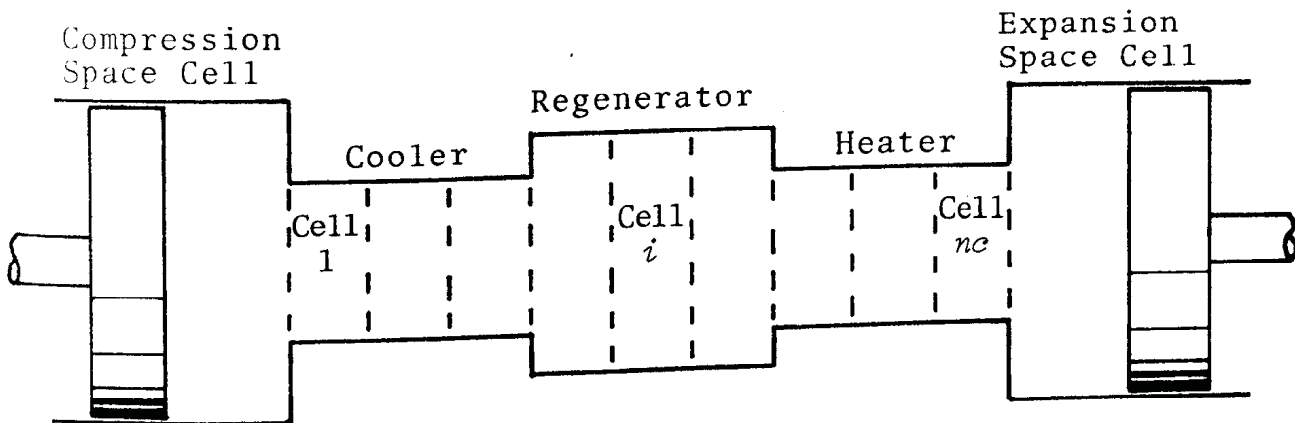


Figure 2.6 The Cellular Model (after Urieli [Ur77])

Viscous friction was accounted for empirically by way of a friction factor selected locally for each cell depending on the local Reynolds' number (the quasi-steady assumption). Heat transfer was calculated from the simple Reynolds' analogy which relates the local heat transfer coefficient to the local friction factor.

Kinetic energy of the working gas and the variation of viscosity with temperature and heat conduction in the machine wall was included in the simulation.

The analytical method adopted was to simplify the system into a one-dimensional model. In one-dimensional flow systems it is impossible to mathematically determine the viscous friction and heat transfer which are strictly three-dimensional effects. Urieli thus used empirical factors to determine the three-dimensional effects.

Four equations describe the gas in each cell, the three transport equations and the equation of state. It is therefore possible to solve for the four parameters which describe the thermodynamic state of the gas. These parameters are: v - the velocity, p - the pressure, T - the temperature and ρ - the density. Urieli related the motion of the gas to g - the mass flux density rather than velocity, and instead of density he used the specific volume v .

The energy of the solid portion in each cell is described by the heat energy conducted in and the thermal capacity of the solid. The conduction is described by the Fourier equation.

A generalised cell was thus formulated as shown in Figure 2.7.

The full description of the generalised cell given by Urieli is as follows:

The i 'th elemental cell consists of a void space having a void volume V_i and containing working gas of mass m_i , temperature T_i , pressure p_i and specific volume v_i (or density ρ_i).

The working gas in this void space is in intimate open communication with the porous cell matrix. The matrix presents a wetted area $A_m g_i$ to the working gas, allowing heat Q_i to be transferred by convection from the matrix to the working gas. The cell axial length is Δx_i . Cell i is bounded by node i being the interface to adjacent cell $i-1$, and node $i+1$ being the interface to adjacent cell $i+1$. The mass flux density g_i across node i through the free flow area A_i gives a total mass flux G_i . The various working gas properties are defined as being constant throughout the cell and discontinuous at the nodes. Thus the node temperature T_{n_i} and the node specific volume v_{n_i} are conditional variables, taking on their respective upstream adjacent cell values, conditional on the direction of mass flux density g_i . Thus referring to the arbitrarily defined positive

direction of flow given in Figure 2.7 (which has been adhered to throughout) one obtains:

$$\begin{aligned}
 g_i \geq & \Rightarrow T_{n_i} \leftarrow T_{i-1}, \quad v_{n_i} \leftarrow v_{i-1} \\
 g_i < & \Rightarrow T_{n_i} \leftarrow T_i, \quad v_{n_i} \leftarrow v_i
 \end{aligned}
 \tag{2.4}$$

where the symbols \Rightarrow and \leftarrow take on their usual mathematical connotations of 'leads to' and 'is replaced by' respectively.

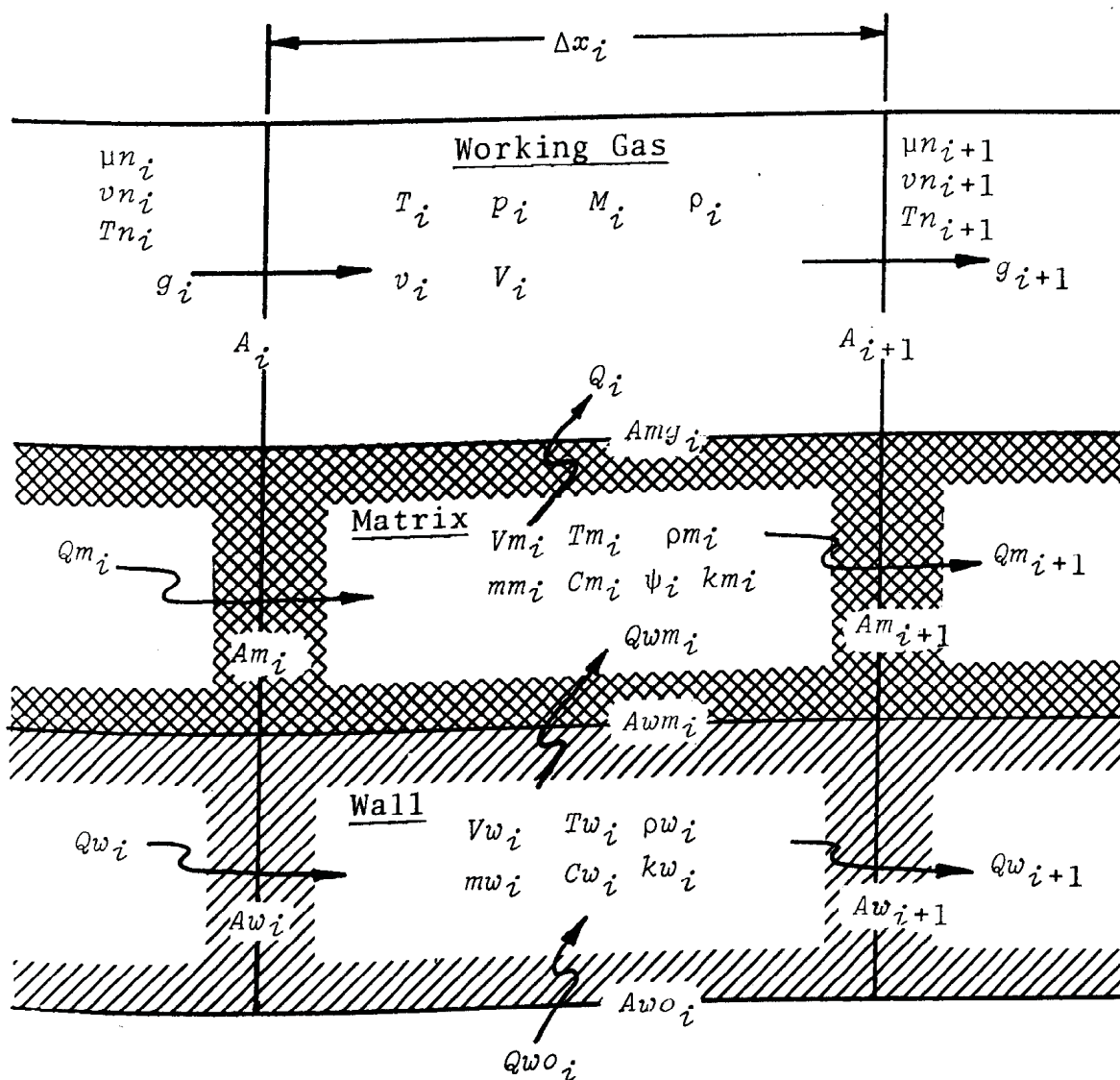


Figure 2.7 The Generalised i 'th Elemental Cell (After Urieli [Ur77])

The cell matrix properties are defined in terms of its overall volume (being the void volume V_i plus the volume occupied by the matrix material Vm_i), porosity ψ_i , density of the matrix material ρm_i , mass mm_i , heat capacity Cm_i , thermal conductivity km_i and temperature Tm_i . Heat transfer by conduction between adjacent cell matrices Qm_i takes place at node i through the matrix effective cross sectional area Am_i . Heat transfer by conduction Qwm_i takes place between the matrix and containing wall through the effective area of contact Awm_i .

The containing wall associated with the i 'th cell has its properties defined in terms of its volume Vw_i , density ρw_i , mass mw_i , heat capacity Cw_i , thermal conductivity kw_i and temperature Tw_i . Heat transfer by conduction between adjacent cell walls Qw_i occurs at node i through the wall cross sectional area Aw_i . Heat transfer with the external environment adjacent to the wall of the i 'th cell, Qwo_i , takes place through the external wall area Awo_i .

The variable volume working space was treated similarly except that an irrecoverable pressure drop (Δp) was defined at the inlet/exit of this space. This was to be evaluated empirically.

The mechanical work W done on the external environment by virtue of a change in volume was assumed to be reversible.

The application example chosen by Urieli was a hypothetical engine of the horizontally opposed configuration in which the working spaces communicated by way of a bundle of stainless steel tubing. For the sake of simplification, adiabatic working spaces were chosen and the pipes were consecutively cooled, insulated and heated. No regenerator matrix was used, regeneration was assumed to take place directly to the tube walls. Figure 2.8 indicates the arrangement schematically.

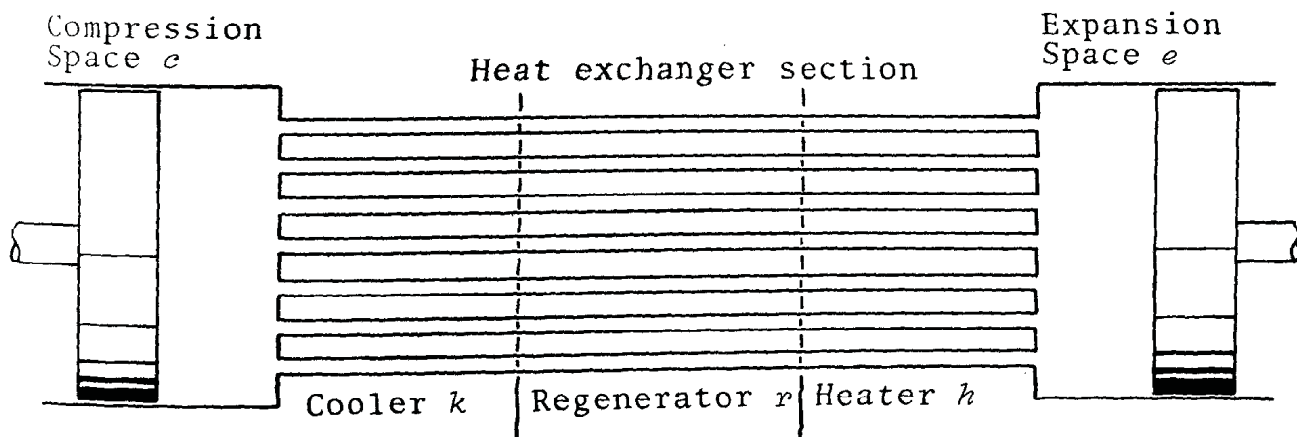


Figure 2.8 The Test Engine (after Urieli [Ur77])

The heater and cooler walls were maintained isothermal at the upper and lower temperatures respectively.

The selection of friction factors pose a special problem to this type of analysis. Generally friction factors are presented for isothermal, incompressible and steady flow conditions. In Stirling machines these conditions are particularly violated. The quasi-steady approach for the viscous friction goes some way to alleviate this problem; since the flow is mainly turbulent [Ur77], the gas tends to mix well and this serves to somewhat reduce the isothermal requirement. However, the steady incompressible flow requirement indicates that this approach ignores contributions by the normal stresses and thus the friction factor only accounts for the shear stresses (note that the normal stresses are only equivalent to the bulk pressure for steady incompressible flow) [KK58, BS60].

The effect of oscillation on the heat transfer coefficient was not included. Bergles [Be69] gives a complete summary of the work done in this field up to 1969. It appears from this work that the heat transfer coefficient can be considerably increased for high frequencies (up to 90 Hz) for liquids.

Martinelli *et al* [MB43] found no significant change in turbulent heat transfer with pulsations of 0,17 to 4,4 Hz.

The entrance and flow development effects were also not considered by Urieli. Work by Kawamura [Ka77] on transient heat transfer for turbulent flow shows that the quasi-steady solution and experimental results diverge with decreasing Reynolds' numbers. Since the transient heat transfer coefficient requires only five diameters to reach 5% of the steady flow value [SH57], this effect may be considered small in most Stirling machines.

The problem of the time required to converge the solution to cyclically steady state was overcome by introducing an empirical convergence factor. This altered the regenerator temperatures in such a way so as to reduce the cyclic net heat stored in the regenerator from the gas to zero. By this method convergence was possible within five to eight cycles of the crankshaft.

Though Urieli's work was not experimentally validated it was shown to be consistent when compared with the published experimental work of Meijer [Me70]. However, comparison with the pressure profiles presented by Walker [Wa62.1] and Kirkley [Ki63] showed disagreement in the phasing of the compression and expansion space pressure profiles. This discrepancy was not resolved.

In summary, the work presented by Urieli is a further development in the evolution of Stirling machine simulation techniques started by Finkelstein. Urieli has presented an approach which takes into account effects which have never before been included in Stirling machine analyses published in the open literature. A successful effort was also made to reduce the computational time which has plagued such approaches in the

na

2.7 Statement of the Problem

Analytically, Urieli's simulation model is more complete than that of Finkelstein. However, Urieli was forced to make certain simplifying assumptions so that the analysis would be more tractable.

The effect of these assumptions must be established, either experimentally or analytically, to give Urieli's work full credibility.

To investigate these assumptions the following activities will be conducted:-

- 1) A critical appraisal of Urieli's analysis.
- 2) A comparison of the simulation model with ideal second order analyses.
- 3) A comparison of the simulation model with experimental work.

Any improvements which become evident in the course of this work will be indicated and if possible be directly included.

3 THE SYSTEM MODEL

3.1 Introduction

The classification of Stirling machine mechanical arrangements are generally divided into three groups, the alpha, beta and gamma configurations [Ki62].

Alpha machines are dual piston or double acting piston arrangements (Figure 3.1). This class includes Rider (1875), De Brey (1947) and the more modern swash plate engines developed by Philips, General Motors and Ford. The principal characteristic of alpha machines is that pistons are used to effect compression, expansion and the approximate constant volume displacement processes.

Beta and Gamma machines on the other hand use a single piston for all processes that involve a change in volume, ie, compression and expansion. The constant volume processes are achieved by way of a displacer or transfer piston (Figures 3.2 and 3.3). Beta machines have the displacer and piston in the same cylinder (Figure 3.2), whilst gamma arrangements employ separate cylinders for the piston and the displacer (Figure 3.3).

The beta class includes one of Stirling's own designs (1816) Lehmann's (1866), and one of Ericsson's designs (1880). More recently, the Philips machine by Rinia (1946) and the Beale free piston engine (1969) belong to this class as well.

The Lehmann engine was in fact the configuration for which the classical Schmidt theory was developed (Appendix A).

The gamma class also includes some of Stirling's own designs (1815 and 1840). The Laubereau (1862) and Hienrici (1884)

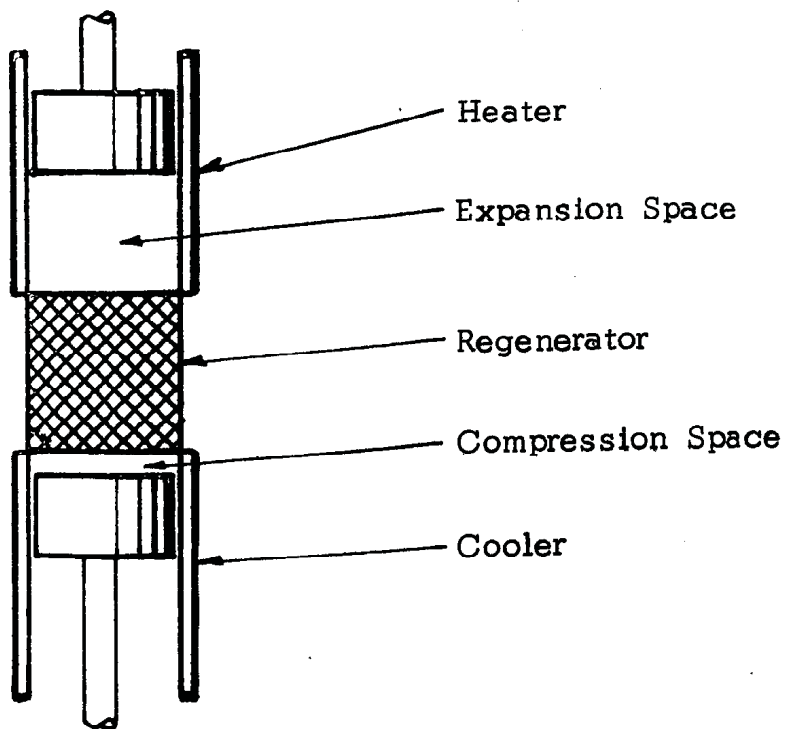


Figure 3.1 Alpha Arrangement

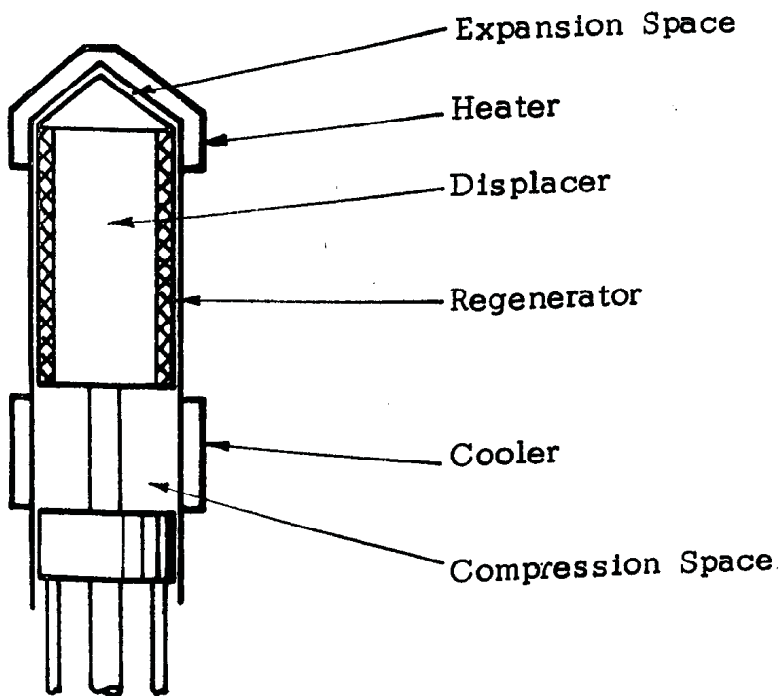


Figure 3.2 Beta Arrangement

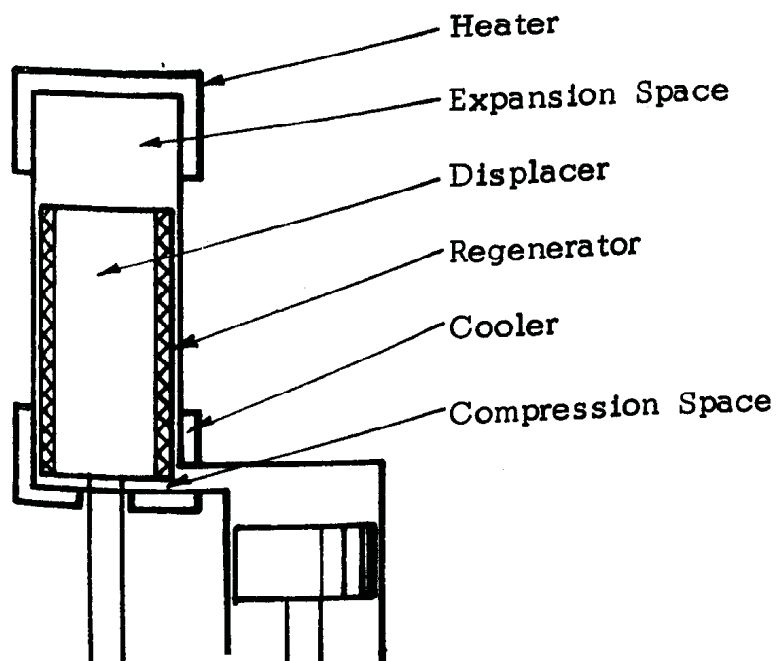


Figure 3.3 Gamma Arrangement

type engines also belong to this category.

From Figures 3.1, 3.2 and 3.3, it can be seen that heat is added and extracted directly at the working spaces. For high power machines it is generally impractical to add and extract all external heat at the working spaces. The main reason for this is simply the limited surface area available for heat transfer to take place. Thus it has become common practice in recent times to add separate hot and cold heat exchangers immediately adjacent to their respective working spaces. In these situations it is often the case that the working spaces play no real role as heat exchangers and it is therefore possible to assume that they are adiabatic [WK65].

A machine in which the major portion of the heat transferred is effected in separate heat exchangers is known as the pseudo-Stirling cycle. An ideal analysis of this cycle (Appendix B) with perfectly adiabatic working spaces indicates that Carnot efficiencies are *not* obtainable. An example of an alpha configuration pseudo-Stirling machine is shown in Figure 3.4.

The configuration chosen for simulation in this work is the alpha pseudo-Stirling arrangement. Thus separate hot and cold heat exchangers are included. It would be possible to define a bulk heat transfer coefficient for the working spaces, however, owing to the lack of empirical information on such heat transfer coefficients, all simulation efforts presented here will be evaluated for adiabatic working spaces.

The experimental rig used for the validation of the model will obviously not have perfect adiabatic conditions in the working spaces. However, the heat transferred at the working spaces was assumed to be small compared with the heat transferred at the hot and cold heat exchangers.

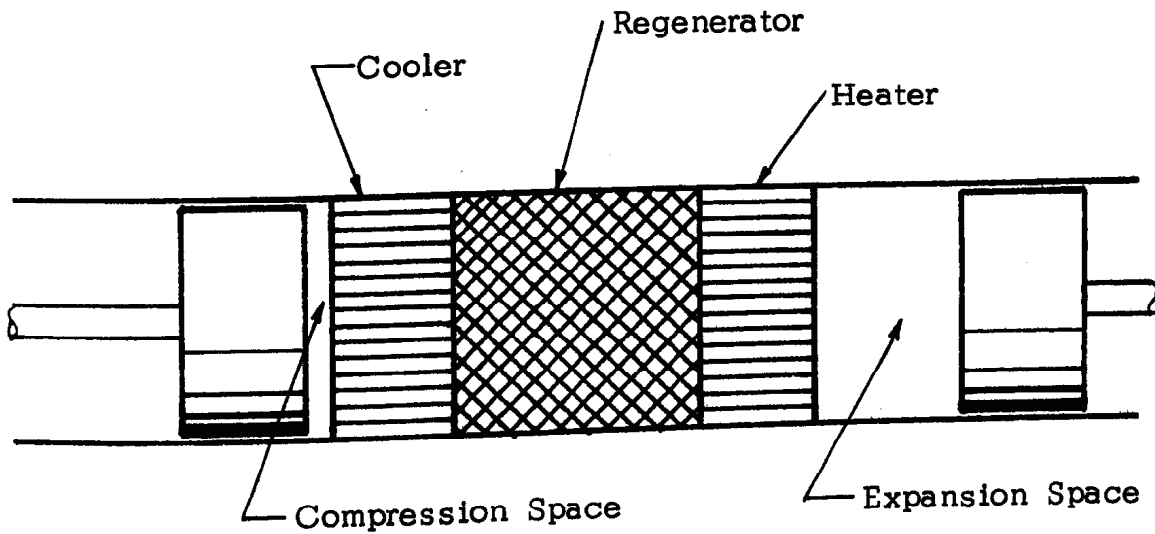


Figure 3.4 The Pseudo-Stirling Machine (Alpha Configuration)

It would be quite feasible to define an arbitrary heat transfer coefficient for these spaces. This heat transfer coefficient could then be used as a 'fudge' factor and be adjusted so that the simulation and experimental results agree as closely as possible. There are obvious objections to such an approach and it was therefore decided that any parameters used in this work must have either analytical or experimental justification. In this way both the power and the limitations of the analytical approach can be better appreciated.

3.2 Numerical Simulation Techniques

It is important to note that there are two basic approaches for simulating complex systems such as Stirling machines. The first method is to write down the governing partial differential equations which describe the system as a continuum. If there is an axis of symmetry in the system it

is often possible to simplify the equations to a minimum two-dimensional system. Similarity and order of magnitude arguments are very powerful in such approaches [Sc68], since they help to indicate which terms in the differential equations are of 'order small', and therefore make little contribution to the overall solution. These terms can then be neglected to further simplify the equations.

The final simplified set of differential equations must invariably be solved by numerical techniques. The spatial derivatives would be discretised into their finite difference forms, and the time derivatives may either be discretised or left in differential form when they exist only in first order format. The resulting set of finite difference equations may then be solved using either explicit or implicit numerical techniques depending on the problem.

For Stirling machine simulation such an approach would require that both laminar and turbulent regimes be accurately modelled in two dimensions. Added complications are that the flow must be considered compressible and non-steady.

This implies that very few simplifications would be possible on the governing differential equations (continuity, momentum and energy). The final simulation procedure would require discretisation both normal to and along the flow direction. Each point in the fluid system would require five equations (assuming two-dimensional flow) for solution. These would be continuity, one momentum equation for each spatial coordinate, the energy equation and the equation of state for the working medium. In addition, since such systems are extremely sensitive to round-off error, it would therefore be imperative that double precision calculations be employed.

Notwithstanding the complexity of such an approach, it can be seen that considerable computer storage and time would be required. Thus each simulation run would be extremely expensive, and the inflexibility in attempting to simulate various machines without too much alteration to the basic programme is a definite disadvantage.

The second method of simulating Stirling machine systems is the technique suggested and used by Urieli [UR77, Ur77]. This method is known as the cellular or concatenated model.

Instead of describing the system in terms of a continuum, the system is broken down into individual discrete cells. Each cell is treated as a separate control volume which can be represented by properties which are continuous in time, but spatially constant over the cell at their spatial mean values. The three transport equations and the equation of state are used to describe each cell in such a way that all the cells are linked consecutively by mass, momentum and energy fluxes. This process of linking the cells together suggests a concatenation, hence the name.

Such an approach can however not be used to determine local rates of heat transfer or the local viscous stresses on the fluid. All these effects (which are strictly three-dimensional) are accounted for by way of empirical coefficients such as heat transfer coefficients and friction factors. The system is thus in effect described by a one-dimensional set of equations.

This implies that only four equations are required per cell to describe the working medium. The two empirical functions for the friction factor and heat transfer coefficient are part of the momentum and energy equations respectively.

The resulting system for solution is thus considerably less complicated than the continuum approach, and in addition, the one-dimensional nature allows easy modification for different machines.

A further advantage of the cellular model over the continuum model is that even when defining each heat exchanger to have only one cell, the resulting system still makes theoretical sense and is solvable [Ur77]. On the contrary it is not possible to make any sense out of the continuum model using one finite difference node in each heat exchanger. This characteristic enables the cellular model to be easily programmed for a variable number of cells. It is thus possible to simulate machines using the minimum number of cells for acceptable accuracy.

The major disadvantage of this approach is that empirical factors which can be used for compressible, non-isothermal and non-steady flow are difficult to come by and are often not documented.

In general it will be necessary to use incompressible, isothermal and steady flow empirical factors for lack of the proper coefficients. Therefore the analysis should be conducted in such a way that these coefficients can be used to their best advantage.

In this work the cellular or concatenated model is used. The so-called integral form of the transport equations is used to describe each cell in the system. The differential equations for a continuum are also derived for comparison. This procedure helps to identify the empirical factors more clearly, and indicates the structure of certain terms which would not otherwise be apparent.

The effects of turbulence are not analytically investigated in this work except in so far as applying turbulent friction factors and heat transfer coefficients where necessary. A short qualitative discussion on turbulence is however included in Appendix D.

5.5 A Critical Investigation of Urieli's Analysis

In this section the mathematical structure of Urieli's work [Ur77, UR77] is investigated in detail.

Urieli derives the fundamental transport equations by considering a control volume as shown in Figure 3.5.

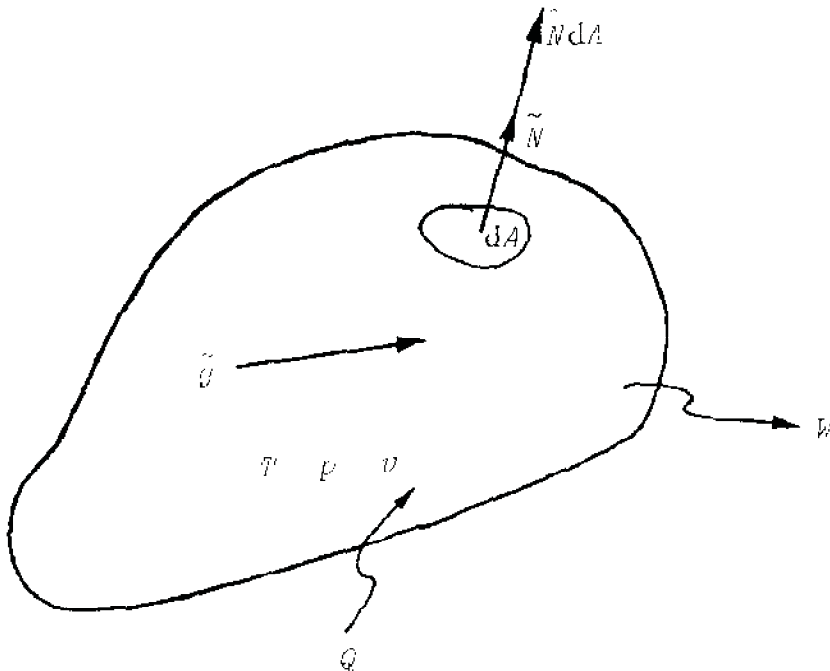


Figure 3.5 The Control Volume

The word statements of each of the three transport equations (continuity, momentum and energy) are written down. This is immediately followed by the equivalent mathematical form. Gauss' theorem is used on all the area integrals (ie, the flux terms) to convert them to volume integrals.

Urieli then makes the assumption that all the fluid parameters are considered to be either [spatially] constant or represented by their [spatially] mean values throughout the control volume. This evidently implies that the integrands are also spatially constant in the same manner as the parameters. All parameters are allowed to vary continuously in time.

Urieli then integrates each equation over the control volume to finally derive the following forms of the transport equations (in normalised form):

Continuity:

$$\frac{\partial m}{\partial t} + V \frac{\partial g}{\partial x} = 0 \quad (3.1)$$

Momentum:

$$\frac{\partial}{\partial t}(g \cdot V) + V \frac{\partial}{\partial x}(g^2 \cdot v) + V \frac{\partial P}{\partial x} + F = 0 \quad (3.2)$$

Energy:

$$\frac{dQ}{dt} = \frac{\partial}{\partial t} \left(\frac{m \cdot T}{\gamma - 1} \right) + V \frac{\partial}{\partial x} \left(\frac{\gamma T \cdot g}{\gamma - 1} \right) + \frac{dW}{dt} - g \cdot v \left(V \frac{\partial P}{\partial x} + F \right) \quad (3.3)$$

where F and dQ/dt are the viscous friction and the convective heat transfer respectively which are determined empirically.

dW/dt is the reversible mechanical work by virtue of a volume change.

For a constant volume cell (ie, $dW/dt = 0$), he shows that the momentum and energy equations may be simplified to the following form:

Momentum:

$$\frac{\partial g}{\partial t} + 2g v \frac{\partial g}{\partial x} + g^2 \frac{\partial v}{\partial x} + \frac{\partial p}{\partial x} + \frac{F}{V} = 0 \quad (3.4)$$

energy:

$$\frac{dg}{dt} = \frac{V}{\gamma - 1} \frac{\partial p}{\partial t} + \frac{V\gamma}{\gamma - 1} \frac{\partial}{\partial x}(Tg) - g v \left(V \frac{\partial p}{\partial x} + F \right) \quad (3.5)$$

The respective finite difference forms for constant volume cells as presented by Urieli are as follows (referring to Figure 2.4):

Continuity:

$$Dm_i = A_i g_i - A_{i+1} g_{i+1} \quad (3.6)$$

Momentum (unequal adjacent cells):

$$Dg_i = 2g_i v n_i (\Delta g / \Delta x)_i + 2g_i^2 (v_{i-1} - v_i) / (\Delta x_{i-1} + \Delta x_i) + \Sigma R_i \quad (3.7)$$

where

$$\Sigma R_i = 2(p_{i-1} - p_i) / (\Delta x_{i-1} + \Delta x_i) - F_i$$

$$v_i \geq 0 \Rightarrow v n_i = v_{i-1}, \quad T n_i = T_{i-1}, \quad (\Delta g / \Delta x)_i = (g_{i-1} - g_i) / \Delta x_{i-1}$$

$$v_i < 0 \Rightarrow v n_i = v_i, \quad T n_i = T_i, \quad (\Delta g / \Delta x)_i = (g_i - g_{i+1}) / \Delta x_i$$

R_i is the viscous resistance evaluated at node i . This term is not relevant to the present discussion therefore its empirical and numerical forms are excluded for the time being.

energy:

$$E_{i+1} = (\gamma - 1) [DQ_i + (A_i g_i Tn_i - A_{i+1} g_{i+1} Tn_{i+1}) \gamma / (\gamma - 1)] / v_i$$

$$= (\gamma - 1) (g_i v n_i \Sigma F_i + g_{i+1} v n_{i+1} \Sigma F_{i+1}) / 2 \quad (3.8)$$

where vn_i , Tn_i , ΣF_i are given in equation (3.7). DQ_i is evaluated empirically.

Referring to the continuity equation (3.1), the simplest central difference form of this equation would be [Ge70]:

$$Dm_i = -v_i (g_{i+1} - g_i) / \Delta x_i \quad (3.9)$$

The truncation error in this approximation is $O(\Delta x_1^2)$.

Comparing (3.9) to the difference formula that Urieli used, i.e., (3.6), it is noticed that Urieli's formula does not agree with the standard difference formulae. Whereas (3.9) approximates a local derivative, Urieli's formula is a determination of accumulating quantities.

However, it can be shown that the finite difference form of the continuity equation given by Urieli does conserve mass, whereas the standard finite difference form in (3.9) does not.

Urieli presented the following result to justify his discretisation technique:

Since the total mass of gas in the system is constant, its time derivative must be zero, hence:

$$Dm_c + Dm_e + \sum_{i=1}^{nc} Dm_i = -A_1 g_1 + A_{nc1} g_{nc1} + \sum_{i=1}^{nc} (A_i g_i - A_{i+1} g_{i+1})$$

$$= 0 \quad (3.10)$$

where Dm_e and Dm_c are the rates of change of the gas masses in the working spaces.

Performing this exercise on equation (3.9) gives the following result:

$$\begin{aligned}
 Dm_e + Dm_c + \sum_{i=1}^{nc} Dm_i &= -A_1 g_1 + A_{nc1} g_{nc1} - \sum_{i=1}^{nc} v_i (g_{i+1} - g_i) / \Delta x_i \\
 &= 0 \quad (A_i = A, \quad i = 1, 2, 3, \dots) \\
 &\neq 0 \quad (A_i \neq A, \quad i = 1, 2, 3, \dots)
 \end{aligned}
 \tag{3.11}$$

Thus (3.9) is only conservative under the condition of constant free flow area throughout the machine.

For the momentum equation, Urieli sticks to standard finite difference formats except in so far as the 'upwind' difference is concerned. This is a standard technique used to avoid instability in unsteady flow systems [Ro72]. The upwind or upstream difference uses a backward difference formula which is conditional on the direction of flow. The backward difference is thus always taken in the upstream direction.

The energy equation is again not discretised according to standard finite difference formulae as can be seen by comparing (3.5) with (3.8). Urieli recognised that the second term on the right hand side of (3.5), ie, $v \frac{\gamma}{\gamma - 1} \frac{\partial}{\partial x} (T g)$, is obviously the enthalpy flux and must therefore be related to the respective flow areas for inflow and outflow. In contradistinction, the pressure derivative is discretised using a standard central difference.

Urieli gave no reasons for the discretisation procedure that he used other than that the numerical results were stable and consistent. Furthermore, the discrepancies between the finite difference formulae and the derivatives they were meant to replace were also not explained.

It appears, therefore, that an intuitive approach was adopted for the discretisation of the derived transport equations. Where the physical interpretation of a particular term was evident, intuitive judgement would be used. The final form of the momentum equation as derived by Urieli is difficult to interpret term by term and here standard finite difference expressions were used.

An anomaly now arises: if the continuity equation had to be discretised as shown by (3.6) for it to be conservative, then it strongly suggests that the finite difference form used for the momentum equation is unlikely. This does not imply that the momentum equation should simply be rediscritised in the same manner as the continuity and energy equations, as the discretisation used for these equations was not mathematically justified.

Since the standard finite difference formulae are derived from a truncated Taylor's series expansion [Ge70] and are therefore mathematically justified as an approximation to the local derivative, there appears little reason to doubt the validity of these formulae. This, however, does imply that Urieli's differential equations may not be rigorous and thus a closer examination of these equations is warranted.

Note that for systems which do not experience area changes, the discretisations given by Urieli all reduce to standard finite difference formulae. In these cases, since all the flow area terms are equal, they may be represented by $V_i/\Delta x_i$, $i = 1, 2, 3, \dots$. For example the continuity equation (3.6) becomes:

$$\Delta m_i + A(g_{i+1} - g_i) + V_i(g_{i+1} - g_i)/\Delta x_i \quad (3.12)$$

Urieli simulated a hypothetical engine which had a constant free flow area throughout. Thus the problem of discretising the system consistently in terms of the above arguments never arose.

3.4 The Fundamental Transport Equations

In this section the basic transport equations are derived both in the integral or macroscopic form and in the differential form.

The integral or macroscopic equations are based on integral balances for a general control volume. An integral balance is defined as an equation in which accumulation is described in terms of the inflow and outflow of any quantity [S172]. Integral equations thus enable the control volume to be treated as a complete entity without being concerned with the detailed behaviour of the fields within the control volume. The resulting expressions are generally relatively simple differential equations for non-steady systems, for steady systems they reduce to simple algebraic expressions. However, it is important to heed Slattery's warning on their use.

....their simplicity is misleading in that one is often forced to make a series of approximations based upon intuitive judgements or related experimental knowledge. It becomes more difficult to say whether a particular analysis will describe an experimental observation within a prescribed error [S172].

The differential transport equations on the other hand describe the system as a continuum. Thus inflow and outflow terms are reduced by the differential calculus to the rates of change of the various parameters in the flow field. The resulting equations describe the variations of the continuum properties at any point and instant in space and time. This approach makes a minimum number of assumptions (it is not possible to make no assumptions when modelling any physical system) and can describe internal processes such as dissipation, whereas the integral approach cannot.

As indicated in Section 3.2 the differential transport equations are extremely difficult to solve except for the most simple systems. They are however very powerful when qualitatively used for discussing interrelated processes in a system. In this way they can be used in conjunction with the integral approach to investigate exactly what assumptions and simplifications are being made by the integral approach.

In this work the differential and integral transport equations are derived and discussed in Appendix D. Only the final form of the integral equations are presented here (in dimensional form):

Continuity:

$$\frac{dm}{dt} = (g A)_i - (g A)_e \quad (D.3)$$

Momentum:

$$\frac{d}{dt}(g V) = (g^2 v A)_i - (g^2 v A)_e + (p A)_i - (p A)_e - F \quad (D.8)$$

where F is the total force on the solid surfaces.

Energy:

$$\begin{aligned} \frac{dQ}{dt} = & \frac{R}{\gamma - 1} \frac{d}{dt}(m t) - \frac{\gamma R}{\gamma - 1} [(T g A)_i - (T g A)_e] \\ & + [(p A g v)_i - (p A g v)_e] - p [(A g v)_i - (A g v)_e] - E \end{aligned} \quad (D.48)$$

where E is the internal dissipation work and dQ/dt is the convective heat transfer.

Note that in the above equations i refers to inflow and e refers to outflow conditions.

It can be seen that the final form of the integral equations are automatically first order simultaneous differential equations.

The discretisation method for these equations is presented in Appendix H. For the sake of example, the final form of the discretised equations for a fixed volume cell is presented here:

For a fixed volume cell the momentum and energy equations are reduced to the following normalised forms (Appendix H):

$$\frac{dg}{dt} = \frac{1}{V} \{ (g^2 v A)_i - (g^2 v A)_e + A(p_i - p_e) \} - F/V \quad (\text{H.7})$$

$$\begin{aligned} \frac{dQ}{dt} = & \frac{V}{\gamma - 1} \frac{dp}{dt} - \frac{\gamma}{\gamma - 1} [(T g A)_i - (T g A)_e] + [(p A g v)_i - (p A g v)_e] \\ & - P [(A g v)_i - (A g v)_e] - E \end{aligned} \quad (\text{H.23})$$

Note that P is the viscous forces only. The pressure force term in the momentum equation (H.7) is different from that in (D.8). The reason for this is that the pressure forces on the solid surfaces have been included in this term. The area in this term is taken to be the smallest flow area of the cell. The full rational argument is included in Appendix E.

Two discretised forms are presented for the momentum equation, one using an 'upstream' difference and the other using a 'central' difference.

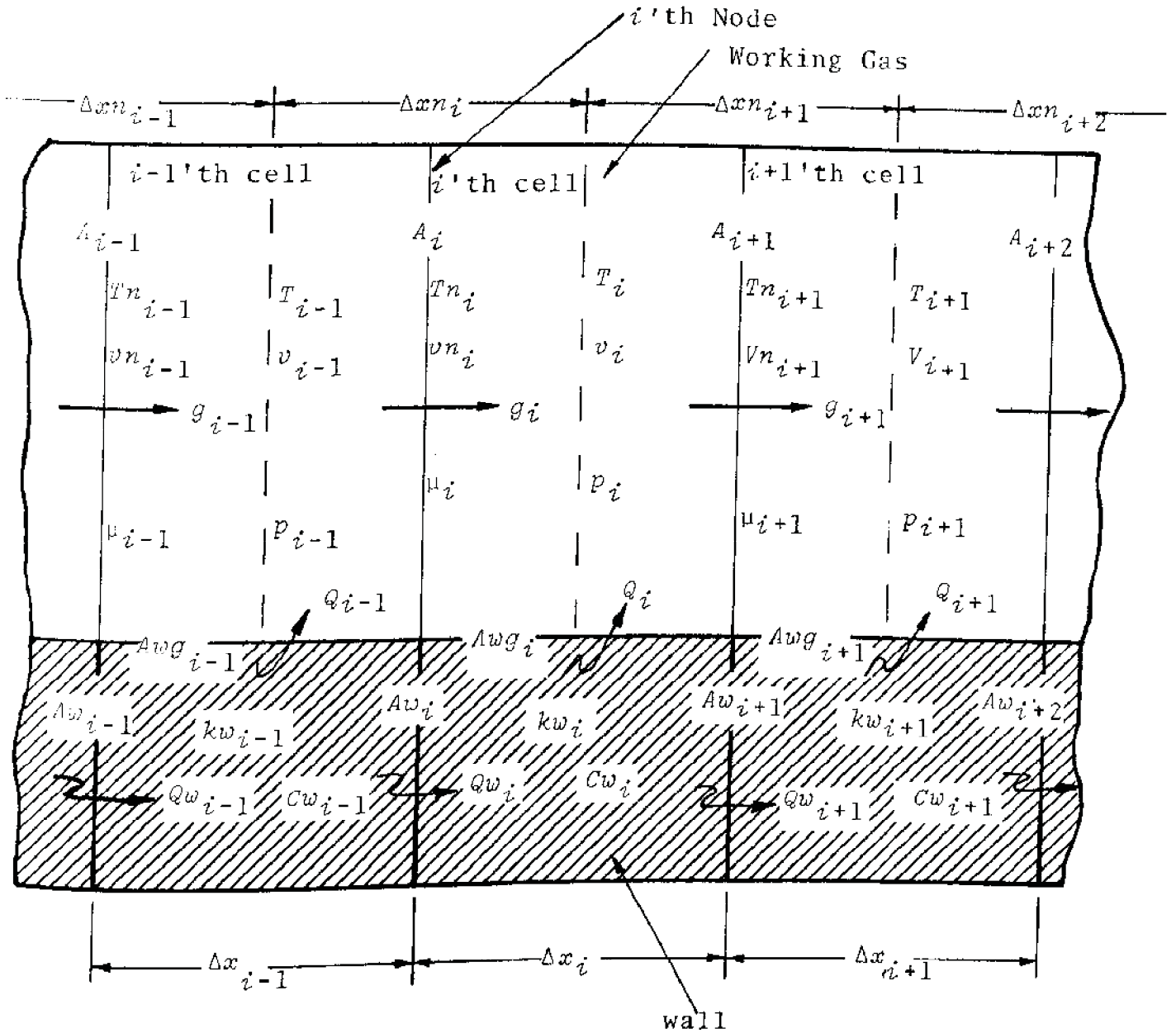


Figure 3.6 The Generalised i'th Cell

Referring to Figure 3.6, the discretised transport equations for a constant volume cell are:

$$Dm_i = A_i g_i - A_{i+1} g_{i+1} \quad (H.1)$$

Momentum (upstream difference):

$$Dg_i = \Delta(g^2 v A)_i / V n_i + (p_{i+1} - p_i) / \Delta x n_i - F_i \quad (H.8)$$

where

$$g_i \geq 0 \Rightarrow v n_i + v_{i-1}, T n_i + T_{i-1},$$

$$\Delta(g^2 v A)_i + (g_{i-1}^2 v n_{i-1} A_{i-1} - g_i^2 v n_i A_i)$$

$$g_i < 0 \Rightarrow v n_i + v_i, T n_i + T_i, \Delta(g^2 v A)_i + (g_i^2 v n_i A_i - g_{i+1}^2 v n_{i+1} A_{i+1})$$

Momentum (central difference):

$$Dp_i + (g_{i-1}^2 v n_{i-1} A_{i-1} - g_{i+1}^2 v n_{i+1} A_{i+1}) / (V_{i-1} + V_i) + (p_{i-1} - p_i) / \Delta x n_i - F_i \quad (H.10)$$

where

$$g_i \geq 0 \Rightarrow v n_i + v_{i-1}, T n_i + T_{i-1}$$

$$g_i < 0 \Rightarrow v n_i + v_i, T n_i + T_i$$

The viscous force in (H.8) and (H.10) will be discussed separately.

Energy:

$$Dp_i + \{ \gamma (T n_i g_i A_i - T n_{i+1} g_{i+1} A_{i+1}) + (\gamma - 1) [DQ_i + (P_i - p_{i+1}) A_i g_i v n_i / 2 + (p_{i+1} - p_i) A_{i+1} g_{i+1} v n_{i+1} / 2 + E_i] \} / V_i \quad (H.27)$$

Comparing the above discretised forms to those developed by Urieli, ie, (3.6), (3.7) and (3.8) the following is noted:-

- 1) The discretised continuity equation derived by Urieli and that derived in the present work are identical.
- 2) If the empirical terms are neglected in both energy equations (since these are open to discussion), then the discretised energy equation derived by Urieli and that derived in the present work are also identical.
- 3) The discretised momentum equations are different.
- 4) As can be seen from Appendix H, no intuitive steps were required for the discretisation of the integral transport equations.

Unfortunately there is no published work in this field against which to compare the discretised momentum equation. However, Schock of Fairchild Industries, Germantown, presented a private communication to Rallis concerning finite difference equations to be used for Stirling machine simulation. Comparing his discretised momentum equation with the central difference momentum equation derived in this work showed them to be identical.

3.5 The Variable Volume Working Spaces

These spaces communicate the work output of the system with the environment. The generalised compression space is shown in Figure 3.7.

The principal assumption made in the working spaces is that the mass flux density g in the working spaces is very much smaller than the mass flux densities in the immediately adjacent heat exchangers. The mass flux density is thus taken to be zero in the working spaces. This creates considerable simplification in the treatment of these cells in that the momentum equation can be completely ignored here. Urieli also

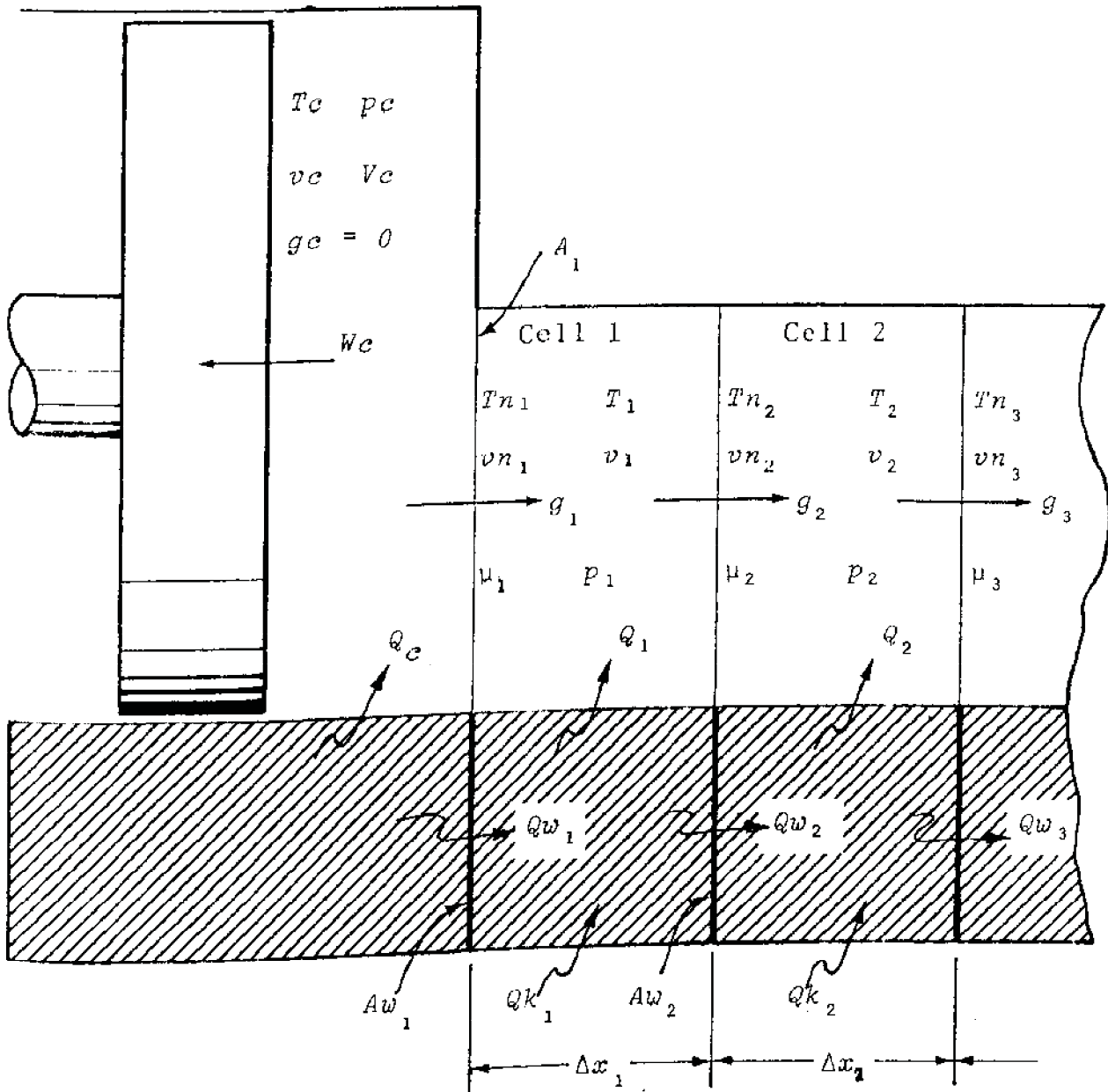


Figure 3.7 The Generalised Compression Space

used this assumption.

The mechanical work done on the piston face is taken to be $p_e dV_e/dt$ for the compression space and $p_i dV_i/dt$ for the expansion space.

The discretisation of the continuity and energy equations for the working spaces is fully described in Appendix H.

3.6 The Empirical Factors

Empirical factors are required to account for the viscous friction F , the dissipation work E and the convective heat transfer dQ/dt .

The friction factors used in this work are taken from standard pipe friction charts (Moody diagrams). As previously noted these friction factors are derived for isothermal, incompressible and steady flow conditions. These conditions are not found in Stirling machines and their relative effects on determining the local friction factor are qualitatively discussed in Appendix E. The effects of compressibility can however be partly accounted for by the inclusion of the normal stresses. These normal stresses are evaluated from the differential momentum equation as outlined in Appendix E.

The result for the viscous resistance so derived is:

$$F = \frac{4}{3}\mu \left\{ \left[A \frac{\partial}{\partial x} (g v) \right]_i - \left[A \frac{\partial}{\partial x} (g v) \right]_e \right\} + 2Fr\mu g V v/d^2 \quad (E.14)$$

Where F_r is the Reynolds' friction factor defined by Urieli [Ur77, UR77] as follows:

$$F_r \triangleq F_f Re \quad (E.15)$$